Since January 2020 Elsevier has created a COVID-19 resource centre with free information in English and Mandarin on the novel coronavirus COVID-19. The COVID-19 resource centre is hosted on Elsevier Connect, the company's public news and information website.

Journal of Molecular Structure 1273 (2022) 134356

Contents lists available at ScienceDirect

Journal of Molecular Structure

journal homepage: www.elsevier.com/locate/molstr

Investigation of embelin synthetic hybrids as potential COVID-19 and COX inhibitors: Synthesis, spectral analysis, DFT calculations and molecular docking studies

Basavarajaiah Suliphuldevara Mathada[a,*], N. Jeelan Basha[b,*], Prashantha Karunakar[c], Ganga Periyasamy[d], Sasidhar B. Somappa[e,f], Mohammad Javeed[g], S. Vanishree[d]

[a] Post Graduate Department of Chemistry, R.V. Road, Vijaya College, Bengaluru 560 004,India
[b] Department of Chemistry, Indian Academy Degree College-Autonomous, Bengaluru 560 043, India
[c] Department of Biotechnology, PES University, Bangalore 560 085, India
[d] Department of Chemistry, Bangalore University, Jnana Bharathi Campus, Bangalore 560056, India
[e] Chemical Sciences and Technology Division, CSIR-National Institute for Interdisciplinary Science and Technology (NIIST), Thiruvananthapuram 695 019, India
[f] Academy of Scientific and Innovative Research (AcSIR), Ghaziabad 201002, India
[g] P. G. Department and Research Studies in Chemistry, Nrupatunga University, Bengaluru 560 001, India

ARTICLE INFO

Article history:
Received 20 July 2022
Revised 28 September 2022
Accepted 16 October 2022
Available online 17 October 2022

Keywords:
ADME
Cyclooxygenase
DFT calculations
Embelin
Molecular docking and SAR study

ABSTRACT

Embelin (2, 5-dihydroxy-3-undecyl-1,4-benzoquinone), a benzoquinone isolated from fruits of Embelia ribes has miscellaneous biological potentials including; anticancer, anti-inflammation, antibiotic, and anti-hyperglycemic activities. Also, embelin down-regulates the overexpression of inflammatory pathways like NF-kB, TACE, TNF-α, and other cytokines. Furthermore, embelin fascinated synthetic interest as a pharmacologically active compound. The present article involves the design, synthesis, DFT calculations, and molecular docking studies of embelin derivatives as cyclooxygenase inhibitors. The structure of these derivatives is confirmed by the various spectral analyses such as IR, NMR, and Mass. The DFT calculations were carried out for the molecules (**1-8**) using CAM-B3LYP hybrid functional with a 6-31+g(d) all-electron basis set using the Gaussian 09 package. Second-order harmonic vibrational calculations are used to check the minimum nature of the geometry. Further, HOMO and LUMO analyses were used for the charge transfer interface between the structures. Based on our previous work and structural activity relationship study, foresaid embelin derivatives were evaluated for in vitro COX-1 and COX-2 inhibitory activity. The compounds **3, 4,** 7, and **8** demonstrated excellent COX inhibitions with IC50 values of 1.65, 1.54, 1.56, and 1.23 μM compared to standard drugs Celecoxib and Ibuprofen. Finally, the molecular docking studies carried out with Covid-19 and cyclooxygenase with all the newly synthesized embelin derivatives.

1. Introduction

The various non-steroidal anti-inflammatory drugs (NSAIDs) are available in the market cures the inflammation, pain and fever (Fig. 1) [1].

The plant *Embelia ribes* commonly known as a false black pepper used for the treatment to fever, inflammation, and gastrointestinal disorders. Further, a bioactive chemical constituent, embelin, has been known for anti-cancer, antimalarial, antimicrobial, and anti-inflammatory activity [2–5] (Fig. 2).

This cell-permeable molecule reduces oxidative stress and inflammation by blocking NF-κB pathways compared to standard anti-inflammatory agents [6–8]. Knowing the importance of the anti-inflammatory potential of embelin, in 2014, Mahendran et al. reported the synthesis of embelin analogs as anti-inflammatory agents [9]. Later, Bezu et al. reported phenazine derivative of embelin as an analgesic and anti-inflammatory agent [10]. Further, Vault et al. reported the synthesis and anti-inflammatory activity of mono, di-acetyl embelin prepared in one step. Their result suggests that these compounds exhibited significant X-linked inhibitors of apoptosis protein (which plays a critical role in cell death and inflammation) inhibition and apoptosis in various cancer cell lines, which is probably independent of inhibition [11,12]. In view of these findings and with the continuation of our research

* Corresponding author.
E-mail addresses: drsmbasu@gmail.com (B.S. Mathada), drjeelan@gmail.com (N.J. Basha).

https://doi.org/10.1016/j.molstruc.2022.134356
0022-2860/

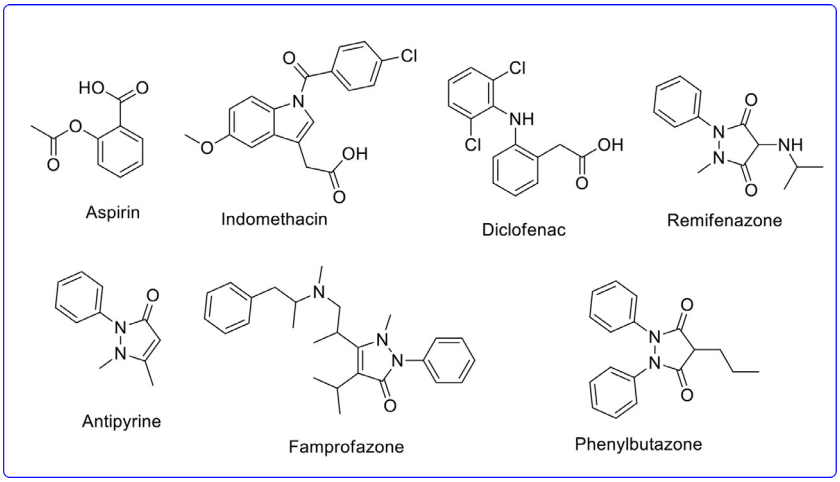

Fig. 1. Various NSAIDs drugs available in the market.

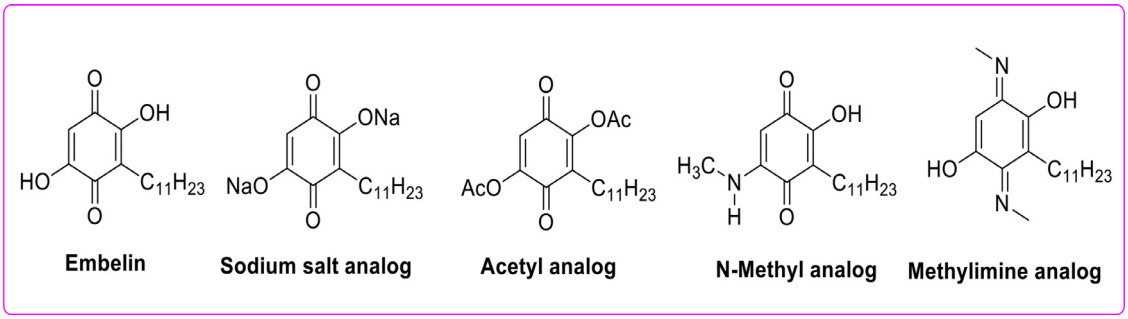

Fig. 2. Embelin and its important analogs reported in the literature.

work on biologically active molecules [13–26], we herein were reporting the synthesis of embelin synthetic hybrids as cyclooxygenase inhibitors and molecular docking studies with SARS-CoV-2 omicron protease & cyclooxygenase enzyme. Initially, embelin was isolated from Embelia ribes fruit by our early reported method. After purification, embelin on treatment with different aliphatic and heterocyclic amines in acidic condition produce targeted compounds (compounds **2**, **3**, **4**, and **8**) in good yield (Scheme-1). The compounds **5**, **6**, and **8** were prepared using reported methods [2,11]. All compounds were purified by column chromatography and characterized by spectral techniques such as IR, NMR, and Mass spectra.

2. Materials and methods

2.1. Instrumentation

On a Perkin-Elmer FT-IR spectrophotometer (Spectrum ONE), (ν_{max} in per centimetre, KBr) were documented, ^{1}H (400 MHz) and ^{13}C NMR (100 MHz) spectra were documented on a Bruker AMX spectrophotometer using DMSO-d_6 as solvent and TMS as an internal standard ESI-mass was recorded on a mass spectrometer equipped with an electrospray ionization source having mass a range of 4000 amu in quadruple and 20,000 amu in Tof. The purity of the compounds was checked using TLC (silica gel 60G F254 plates) and iodine vapors were utilized as visualizing agents. The elemental analysis was carried out using the elemental analyzer Flash EA1112 series.

2.2. Experimental

The chemicals used in the experiments were procured from certified suppliers and used without further purification.

2.2.1. Isolation, purification and characterization of embelin (1)

Isolation of embelin involves slight modification of earlier reported method [2]. Coarsely powdered fruits of *Embelia ribes* (200 g) were exhaustively extracted initially with hexane and then with chloroform by cold extraction method (500 ml). After 48 h, the solvent was decanted and evaporated using a Rota evaporator. The obtained extract was concentrated and subjected to column chromatography over silica gel (100-200 mesh). Elute column with chloroform first then with chloroform and methanol. Collect the fractions of chloroform: methanol (9:1) and evaporating under reduced pressure using Rota evaporator yielded an orange color powder which on crystallization with ether afforded orange plates of embelin (Yield: 1.2 gm). The purity of the compound was monitored by TLC. Isolated embelin was further characterized by spectral data such as ^{1}H,^{13}C NMR and ESI-MS.

2.2.2. Spectral data of embelin (1)

Orange crystals, m. p. 144-145°C, IR (KBr) cm^{-1}: 3320 (OH), 1660 (C=O); ^{1}H NMR (400 MHz, $CDCl_3$) d: 5.221 (s, 1H, H-6), 2.293 (t, 2H, H- 1′), 1.22-1.30 (m, 18H, H-2′, H-3′ to 10′), 0.83 (t, 3H, H-11′). ^{13}C NMR (100 MHz, $CDCl_3$) 14.15 (C-11′), 22.04 to 40.16 (C-1′ to C10′), 99.23 (C-6), 110.01 (C-3), 178.81 (C-2), 181.35 (C-5), 206.37 (C=O). ESI-MS: m/z 295 $[M+H]^+$.

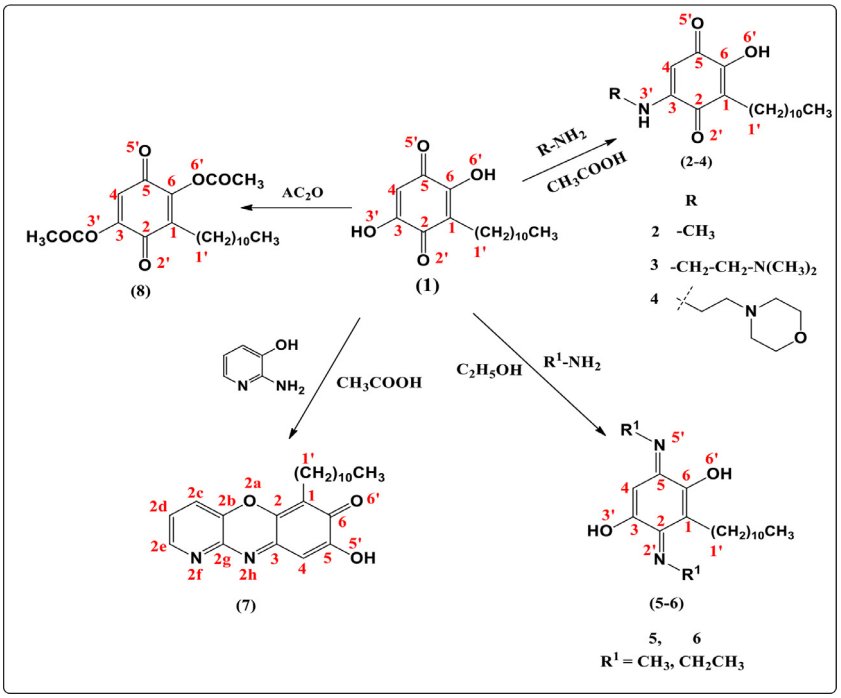

Scheme 1. Synthesis of embelin derivatives.

2.2.3. General procedure for synthesis of embelin amine derivatives(2-4)

Embelin (0.4 mmol) in acetic acid (15 ml) and substituted amines (0.5 mmol) refluxed for 4 hr. Pour the reaction mixture in ice cold water, separated solid was filtered and dried to get the product. The crude product was purified through column chromatography using mobile phase hexane: ethyl acetate (8:2).

2.2.4. 2-Hydroxy-5-(methylamino)-3-undecylcyclohexa-2,5-diene-1,4-dione (2)

Yield: 53%.Brown color solid. m. p.110-111°C. IR (KBr) cm^{-1}: 3330 (NH), 1675 (C=O).^{1}H NMR (400 MHz, DMSO): 7.8 (s, 1H, -OH), 5.2 (s, 1H, H-6), 2.74 (s, 3H, NCH_3), 2.25 (t, 2H, H- 1′), 2.17 (s, 1H, NH), 1.32 (m, 2H, H-2′), 1.226-1.15 (m, 16H, H-3′ to 10′), 0.831 (t, 3H, H-11′); MS (MALDI-ToF, CHCA): m/z 308.09 $[M+H]^+$, calc. 307.27) [2].

2.2.5. 5-(2-(Dimethylamino)ethylamino)-2-hydroxy-3-undecylcyclohexa-2,5-diene-1,4-dione (3)

Yield: 71%. Brown crystals, m. p. 91-92°C, IR (KBr) cm^{-1}: 3321 (NH), 1694 (C=O); ^{1}H NMR (400 MHz, DMSO): 6.99 (s, 1H, -OH), 5.33 (s, 1H, H-6), 3.21 (t, 2H, -NH**CH_2**), 2.63 (t, 2H, -**CH_2**$N(CH_3)_2$), 2.40 (t, 2H, H-1′), 2.30 (s, 6H, $-N(CH_3)_2$), 2.18 (s, 1H, NH), 1.44-1.25 (m, 16H, H-2′ to 10′), 0.85 (t, 3H, H-11′).^{13}C NMR (100 MHzCDCl$_3$) 14.18 (C-11′), 22.93 to 40.78 (C-1′ to C10′), 44.32 (NCH2), 47.67 ($N(CH_3)_2$), 62.47 (N(CH3)$_2$CH2), 102.33 (C-6), 116.21 (C-3), 176.91 (C-2), 181.35 (C-5), 204.81 (C=O). ESI MS: m/z 365 [M+1].Elemental analysis: Calcd for $C_{21}H_{36}N_2O3$: C, 69.19: H, 9.95; N, 7.68. Found: C, 69.14: H, 9.93; N, 7.65.

2.2.6. 2-Hydroxy-5-(4-(2-aminoethyl)morpholino)-3-undecylcyclohexa-2,5-diene-1,4-dione (4)

Yield: 69%. Brownish solid, m. p. 120-121°C, IR (KBr) cm^{-1}: 3390 (OH), 1678 (C=O); ^{1}H NMR (400 MHz, DMSO): 7.40 (s, 1H, -OH), 5.29 (s, 1H, H-6), 4.03 (t, 4H, OCH_2), 2.54 (t, 2H, ring NCH_2), 2.49 (t, 2H, NCH_2), 2.31 (t, 2H, NCH_2), 2.29 (t, 2H, H-1′), 2.17 (s, 1H, NH), 1.38-1.15 (m, 18H, H-2′, H-3′ to 10′), 0.832 (t, 3H, H-11′);^{13}C NMR (100 MHz, $CDCl_3$) 14.1 (C-11′), 22.74 to 40.38 (C-1′ to C10′), 44.90 (NCH_2 {attached to morpholine}), 55.62 (NCH_2 {attached to quinone}), 56.82 (ring NCH_2), 67.72 (ring OCH_2), 103.23 (C-6), 117.01 (C-3), 174.91 (C-2), 180.35 (C-5), 205.31 (C=O). MS (MALDI-ToF, CHCA): m/z 407.21 $[M+H]^+$.Elemental analysis: Calcd for $C_{23}H_{38}N_2O_4$: C, 67.95: H, 9.42; N, 6.89. Found: C, 67.93, H, 9.40; N, 6.86.

2.2.7. Synthesis of (3E, 6E)-3,6-bis(alkylimino)-2-undecylcyclohexa-1,4-diene-1,4-diol (5-6)[2]

To a mixture of embelin (0.34 mmol)) and amines (0.68 mmol) added 10 ml ethanol refluxed for 2 hr. Evaporation of excess ethanol gives crude residue, which is further purified by column purification to obtain the desired compound using mobile phase hexane and ethyl acetate(7:3).

2.2.8. (3E, 6E)-3,6-bis(Methylimino)-2-undecylcyclohexa-1,4-diene-1,4-diol (5)

Yield: 83%.Violet solid, m. p. 89-90°C, IR (KBr) cm^{-1}: 3310 (OH). ^{1}H NMR (400 MHz, DMSO): 8.9 (s, 2H, -OH), 5.23 (s, 1H, H-6), 2.98 (s, 3H, NCH_3), 2.95 (s, 3H, NCH_3), 2.21 (t, 2H, H-1′), 1.26-1.21 (m, 18 H, H-2′, H-3′ to 10′), 0.835 (t, 3H, H-11′); MS (MALDI-ToF, CHCA): m/z 321.14 $[M+H]^+$).

2.2.9. (3E, 6E)-3,6-bis(Ethylimino)-2-undecylcyclohexa-1,4-diene-1,4-diol (6)

Yield: 81%. Purple crystals, m. p. 78-79°C, ^{1}H NMR (400 MHz, DMSO): 7.8 (s, 2H, OH), 5.2 (s, 1H, H-6), 2.74 (q, 3H, N**CH_2**C), 2.71 (t, 3H, NC**CH_3**), 2.20 (t, 2H, H-1′), 1.33 (m, 2H, H-2′), 1.28-1.12 (m, 16H, H-3′ to 10′), 0.82 (t, 3H, H-11′); MS (MALDI-ToF, CHCA): m/z 349.09 $[M+H]^+$.Elemental analysis: Calcd for $C_{21}H_{36}N_2O_2$: C, 72.37, H, 10.41; N, 8.04. Found: C, 72.35, H, 10.36; N, 8.01.

Table. 1
Physiochemical parameters of compounds 1-8 predicted by SwissADME.

Parameters*	1	2	3	4	5	6	7	8
MW	294.39	307.43	364.52	406.56	320.47	348.52	368.47	378.46
NHA	21	22	26	29	23	25	27	27
NAHA	0	0	0	0	0	0	14	0
NRB	10	11	14	14	10	12	10	14
NHBA	4	3	4	5	4	4	5	6
NHBD	2	2	2	2	2	2	1	0
MR	84.31	90.35	107.67	120.17	100.9	110.51	109.75	102.97
TPSA	74.6	66.4	69.64	78.87	65.18	65.18	76.22	86.74
iLOGp	3.28	3.59	4.31	4.59	4.33	4.75	4.04	4.23
Log S (ESOL)	-4.42	-4.65	-4.83	-4.85	-4.81	-5.23	-5.8	-4.82
MLOGP	1.21	1.44	1.3	0.92	1.68	2.13	2.36	1.94
GI	High	High	High	High	High	High	High	High
BBBP	Yes	Yes	Yes	Yes	No	No	No	No
vLROF	0	0	0	0	0	0	0	0
vGR	0	0	0	0	0	1	0	0
vVR	0	1	1	1	0	1	0	1
BS	0.85	0.85	0.55	0.55	0.55	0.55	0.55	0.56
SA	3.66	3.88	4.3	4.42	4.36	4.67	4.02	4.11

* MW: Molecular weight; NHA: Num. heavy atoms; NAHA: Number of aromatic heavy atoms; NRB: Num. rotatable bonds; NHBA: Num. H-bond acceptors; NHBD: Num. H-bond donors; MR: Molar Refractivity; TPSA:Topological Polar Surface Area; Log S: Solubility class; MLOGP: Moriguchi octanol-water partition coefficient: GI: Gastrointestinal absorption; BBBP: Blood Brain Barrier Penetration; vLROF: Violation ofLipinski's rule of five; vGR: Violation of Ghose rule; vVR: Violation of Veber rule; BS: BioavailabilityScore; SA: Synthetic accessibility.

2.2.10. Procedure for synthesis of 8-hydroxy-6-undecyl-7H-benzo[b]pyrido[2,3-e][1,4]oxazin-7-one oxazine (7)

Embelin (0.68 mmol) and 2-amino-3-hydroxypyridine (0.68 mmol) in acetic acid (10 ml) refluxed for 4 hr. Pour the reaction mixture in to ice water. Solid separated was dried and purified with column chromatography using hexane and ethyl acetate as a mobile phase (8:2).

Brown solid,Yield-73 %, m. p. 132-134°C, IR (KBr) cm^{-1}: 3390(OH), 1678 (C=O); ^{1}H-NMR (400 MHz, DMSO): 7.51-7.56 (m, 4H, pyridine-CH, OH), 6.62 (s, 1H, H6), 5.328 (s, 1H, H-6), 2.67 (t, 2H, H- 1′), 1.48-1.15 (m, 16H, H-2′ to 10′), 0.83 (t, 3H, H-11′).^{13}C NMR (100 MHz, $CDCl_3$) 14.21 (C-11′), 22.34 to 40.11 (C-1′ to C10′), 103.55 (C-6), 115.12 (C-3), 121.4, 134.05, 140.05 (Pyridine-C), 149.3 (C=N oxazine), 159.5 (C=N Pyridine), 173.95 (C-2), 181.11 (C-5), 206.81 (C=O).MS (MALDI-ToF): m/z -368, 369$[M+H]^+$, 390 $[M+Na]^+$.Elemental analysis: Calcd for $C_{22}H_2{}_8N_2O_3$: C, 71.71; H, 7.66; N, 7.60. Found: C, 71.69, H, 7.62; N, 7.56.

2.2.11. 3, 6-Dioxo-2-undecylcyclohexa-1,4-diene-1,4-diyl diacetate (8)

A solution of embelin (0.34 mmol) and acetic anhydride (10 ml) refluxed for 1 hour. Cool the reaction mixture, pour in to ice water. Solid separated was dried and recrystallize from ethanol to obtain diacetyl embelin [11].Yield: 72%. Pale yellow solid, m. p. 90-91°C, IR (KBr) cm^{-1}: 1659 (C=O); 1171 (C-O-C).

2.3. Drug like profile

The physiochemical characteristics, ADMETand drug-likeness for molecules are critical in their fundamental unique proof as a synthetic lead and serve as a baseline against which integrated compounds are tested during lead development. The http://www.swissadme.ch/index.php was used to screen the stages of absorption, distribution, metabolism, and excretion of the ligand molecules. Numerous properties like molecular weight, numberof heavy atoms, number of aromatic heavy atoms, number ofrotatable bonds, molar refractivity, topological polar surfacearea, solubility, gastrointestinal absorption, blood–brain,barrier penetration, Lipinski's rule of five, Ghose rule, Veberrule, bioavailability score, and synthetic susceptibility werepredicted (Table 1) [28].The main goal of this study is to estimate the pharmacokinetic characteristics of the substances under investigation.

2.4. In vitro anti-inflammatory activity

Inflammation is a multi-step progression driven by intensely produced arachidonic acid and its metabolic products like prostaglandins. The COX-1 and COX-2 are two cyclooxygenases (COX) isozymes involved in prostaglandin synthesis. In continuation of our previous reported research articles on the anti-inflammatory activity of heterocycles [29–31], herein we report in vitro anti-inflammatory of synthesized compounds via COX-1 and COX-2 inhibition by enzyme immune assay.

2.4.1. COX-1 and COX-2 inhibition by colorimetric assay

The ability of the test compounds listed in Table 1 to inhibit ovine COX-1 and human recombinant COX-2 (IC_{50} value, μM) was determined using an enzyme immuno assay (EIA) kit according to the reported method [32].

2.5. Molecular docking studies

The primary protein structure of SARS-CoV-2 Omicron virus variant (PDB ID:7T9L) and cyclooxygenase-2 (PDB ID:6COX) were obtained from the Protein Data Bank. The 3D structures of a few ligands were obtained from PubChem. The software Chemdraw 12 was used to draw the newly synthesized compounds. 3D structures were loaded into the PyRX 0.9 and energy minimized using the Universal Force Field (UFF) available under the OpenBabel [33]. A molecular docking study of the synthesized compounds and celecoxib and ibuprofen taken as reference was performed using PyRX-0.9.2 software. The ligands were blindly docked using the AutoDock Vina program to identify the compound with the best binding properties. The grid box for 7T9L was set to the XYZ coordinates as 214.866, 163.360, and 254.26 respectively with the centres of XYZ in the positions of 86.869, 84.09, and 122.748, respectively. The docking of the co-crystallized ligand S58 (1-Phenylsulfonamide-3-trifluoromethyl-5-parabromophenylpyrazole) bound to the COX-2 protein was re-docked and the interaction of the ligand with the protein is validated along with the docking procedure. S58 formed three hydrogen bonds along with nine hydrophobic interactions which matches with the PDBSum results for the S58-6COX complex.The grid box for the COX protein was set to the XYZ coordinates as 47.82, 24.69, and 36.44 respectively with the centres of XYZ in the

Table 2
Computed bonding, non-bonding distances, bond angles and dihedrals for the molecules 1-8.

	1		2	3	4	5	6	7	8
Bonding and Non-bonding distances (indicated in*), Å									
C1-C2	1.45		1.45	1.45	1.45	1.35	1.48	1.35	1.48
C1-C1′	1.50		1.50	1.50	1.50	1.50	1.50	1.49	1.49
C1′- H1′	1.09		1.09	1.09	1.09	1.01	1.91	1.09	1.09
C2-C3	1.50		1.51	1.51	1.51	1.48	1.48	1.48	1.49
C2-O2′	1.22		1.21	1.21	1.21	-	-	-	1.20
O2′-H3′*	1.99		2.15	2.14	2.13	-	-	-	-
C2-N2′	-		-	-	-	1.35	1.27	-	-
N2′-C2′	-		-	-	-	1.45	1.45	-	-
C2-O2a	-		-	-	-	-	-	1.35	-
O2a- C2b	-		-	-	-	-	-	1.36	-
C2b-C2c	-		-	-	-	-	-	1.38	-
C2c-H2c'	-		-	-	-	-	-	1.08	–
C2c-C2d	-		-	-	-	-	-	1.38	-
C2d-H2d'	-		-	-	-	-	-	1.08	-
C2d-C2e	-		-	-	-	-	-	1.39	-
C2e-H2h'	-		-	-	-	-	-	1.08	-
C2e-N2f	-		-	-	-	-	-	1.32	-
N2f-C2g	-		-	-	-	-	-	1.33	-
C2g- N2h	-		-	-	-	-	-	1.38	-
N2h-C3	-		-	-	-	-	-	1.29	
C3-C4	1.34		1.36	1.35	1.35	1.34	1.33	1.44	1.32
C3-O3′	1.32		-	-	-	1.35	1.36	-	1.36
O3′- H3′*	0.97		-	-	-	0.96	0.96	-	-
C3-N3′	-		1.34	1.34	1.34	-	-	-	-
N3′-H3′*	-		1.01	1.01	1.01	-	-	-	-
N3′-C3′	-		1.44	1.44	1.44	-	-	-	-
O3′- C3′	-		-	-	-	-	-	-	1.37
C3′- O3′'	-		-	-	-	-	-	-	1.19
C4-C5	1.45		1.44	1.44	1.44	1.45	1.46	1.34	1.47
C4-H4′	1.08		1.08	1.08	1.08	1.08	1.08	1.08	1.08
C5-C6	1.51		1.52	1.51	1.51	1.48	1.48	1.49	1.49
C5-O5′	1.21		1.21	1.21	1.21	-	-	-	1.21
C5-N5′	-		-	-	-	1.27	1.27	-	-
N5′-C5′	-		-	-	-	1.45	1.45	-	-
C5-O5′	-		-	-	-	-	-	1.33	-
O5′-H5′	-		-	-	-	-	-	0.97	-
C6-O6′	1.33		1.33	1.33	1.33	1.34	1.36	1.22	1.37
O6′-H6′	0.96		0.96	0.96	0.96	0.96	0.96	-	1.37
O6′-C6′ C6′-	-		-	-	-	-	-	-	1.19
O6''	-		-	-	-	-	-	-	-
BondAngles in º									
C1C2C3	119.66		119.11	119.11	119.17	115.74	115.51	123.93	118.16
C2C3C4	121.90		120.81	120.78	120.77	122.11	121.62	117.99	122.19
C3C4C5	119.88		121.09	121.10	121.07	122.43	123.71	119.63	120.24
C4C5C6	117.54		117.18	117.18	117.20	115.74	114.70	121.96	117.33
C5C6C1	123.16		123.24	123.25	123.23	122.81	122.79	119.02	123.59
C6C1C2	117.84		118.56	118.55	118.53	121.11	121.55	117.42	118.29
C3O3′H3′	106.31		-	-	114.95	109.64	109.29	-	-
C6O6H6′	110.27		110.07	110.04	110.08	109.28	109.42	-	-
C3N3′H3′	-		115.29	115.13	-	-	126.18	-	-
C3N3′H3′	-		-	-	-	-	125.65	-	-
C2N2′C2′	-		-	-	-	-	-	-	-
C5O5′C5′	-		-	-	-	126.11	-	-	-
C4C3N2h	-		-	-	-	119.84	-	119.37	-
O6′C6C1	-		-	-	-	-	-	124.02	-
C1C2O2a	-		-	-	-	-	-	118.56	-
C4C5O5′	-		-	-	-	-	-	123.99	-
C3O3′C3′	-		-	-	-	-	-	-	116.98
C6O6C6′	-		-	-	-	-	-	-	116.95
Dihedrals in º									
C1′C1C2O2′		1.13	0.78	0.41	1.65	-	0.09	-	6.38
C1′C1C6O6′		-1.04	-0.92	-0.97	-1.07	-	-0.42	-	2.69
C1C6O6′H6′		-0.70	-0.81	-0.94	-0.76	-	-0.42	-	-
C2C3O3′H3′		-0.09	-	-	-	-	179.89	-	-
C2C3N3′H3′		-	-0.26	-1.37	3.12	-	-1.06	-	-
C1′C1C2N2′		-	-	-	-	-0.67	-	-	-
C1′C1C6O6′		-	-	-	-	-0.56	-	0.81	-
C1C6O6′H6′		-	-	-	-	-0.81	-	1.09	-
C2C3O3′H3′		-	-	-	-	-179.8	-	0.03	-
O6′C6C5N5′		-	-	-	-	-0.30	-	0.16	-
C1′C1C202a		-	-	-	-	–	-	-	-
C2C3N2HC2		-	-	-	-	-	-	-	-
O6′ C6 C5O5′			-	-	-	-	-	-	-
C1C6O6′C6′			-	-	-	-	-	-	117.34
C2C3O3′C3′			-	-	-	-	-	-	65.81

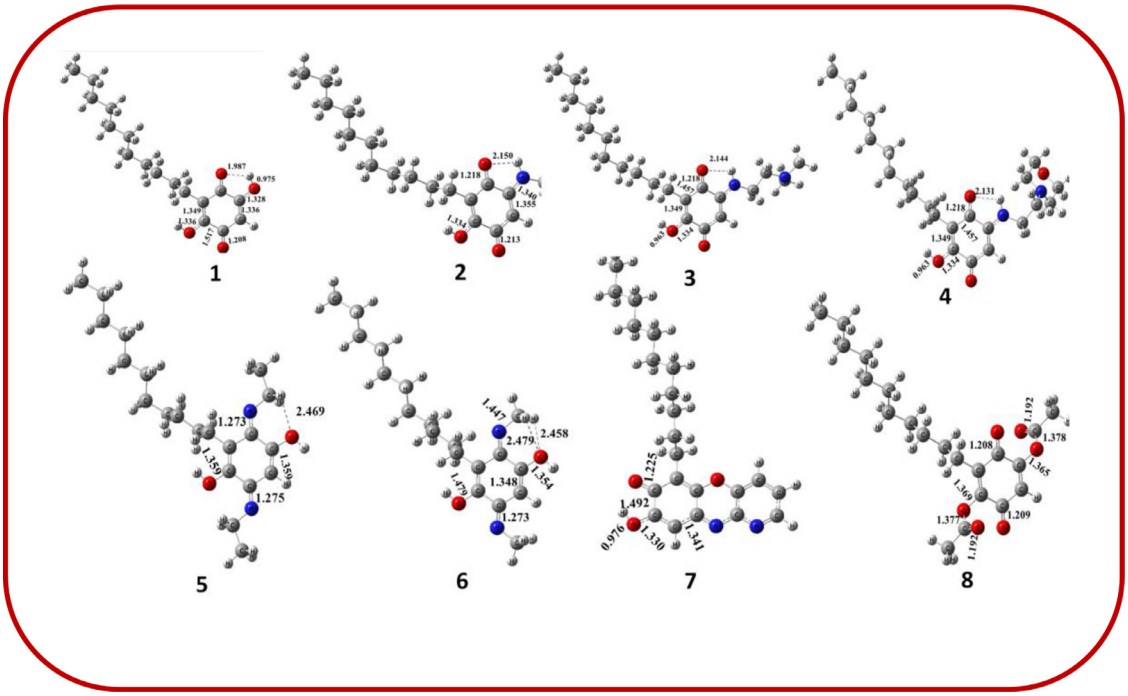

Fig. 3. Optimized geometries of molecules **1-8**.The complete structural parameters are given in the table 2.

positions of 108.49, 77.37 and 77.47, respectively. The nine conformations of each compound along with the Vina score and RMSD value were used to screen for the best binding interaction. The 2D interaction diagrams generated from LigPlot+ were used to analyze the ligand interactions and the 3D interactions were done using PyMOL [34–37].

3. Results and discussion

3.1. Chemistry

The literature suggests Embelia Ribes and their chemical constituent's embelin is known to inhibit NF-κB activity and COX-2 expression, which are related to various inflammation diseases like chronic inflammation, rheumatoid arthritis, atherosclerosis, multiple sclerosis, and asthma. In light of this**,** embelin (2, 5-dihydroxy-3-undecyl-1,4-benzoquinone) subjected to react with different amines in acetic acid obtain compounds (**3** and **4)** in moderate to good yield.

The compound (**3**) formation was confirmed by the new peaks in 1H NMR at δ 2.637-2.364 (t, CH_2, NCH_2), 2.402 (t, 2H, H- 1′), 2.303 (s, 6H, $N(CH_3)_2$), and 2.170 (s, 1H, NH). Further, supported by the presence of a molecular peak of 365 (M+1) in its mass spectra. Compound (**4**) confirmed by ^{1}H NMR showing peaks at δ 4.032 (t, 2H OCH_2), 3.582 (t, 2H OCH_2), 3.163 (t, 2H, ring NCH_2), 2.54 (t, 2H, ring NCH_2), 2.49 (t, 2H, NCH_2), and 2.312 (t, 2H, NCH_2). The formation of molecular ion peak at m/z 407 clearly indicated the formation of compound **4** from embelin. Further, the compounds (**5-6**) were synthesized by using the known method by the reaction of embelin and primary amines in ethanol [2]. Also, cyclization followed by aromatization with 2-amino-3-hydroxy pyridine gives the target compound (**7**) having 73% yield. This cyclization was confirmed by the presence of four aromatic protons at δ7.517-7.562 and mass spectra showing a molecular peak at 368. Finally, the reaction of embelin with acetic anhydride furnished diacetyl embelin (**8**) [11]. The physical data of the newly synthesized compound 8 is agreement with reported one (Scheme-1).

3.2. DFT calculations

The DFT calculations were carried out for the molecules **1-8** using CAM-B3LYP hybrid functional [27a]with 6-31+g(d) all-electron basis set using the Gaussian 09 package. Second-order harmonic vibrational calculations were performed to check the minimum nature of the geometry. The electronic properties chemical hardness [η = (LUMO-HOMO)/2], electronegativity [χ =-(HOMO+LUMO)/2], chemical potential [μ = (H+L)/2], and electrophilicity index ($\omega = \mu 2/2\eta$) were calculated using the energies of Highest Occupied Molecular Orbital (HOMO) and Lowest Unoccupied Molecular Orbital (LUMO). Chemical hardness (η) has been used to understand the molecular system's chemical reactivity [27b-f]. The concept of electronegativity (χ) explains the molecular electron-accepting ability. Electrophilicity (ω) has been proposed as a measure of lowering energy due to maximal electron flow between donor and acceptor. Finally, HOMO-LUMO (Δ) gap establishes the correlation between chemical structure and biological activity.

Vibrational spectral assignments are done at B3LYP/6-31+G(d,p). The structure shows the presence of a single N-H…O and O-H…O intra-molecular H-bonds. In all structures, the aromatic ring is attached to the long alkane chain, which increases the ring C-C bond distance, as shown in Fig. 3 and Table-1. The computed bond distances and stretching frequencies are in good corroboration with the experimental parameters that validates the method adopted here (Table 3).The HOMO and LUMO energy values show the electron-donating and accepting ability of the molecules, respectively Fig. 4). Computed HOMO and LUMO Eigen functions indicate the MOs localized at the aromatic centre, which does not have any contribution from the longer alkane chain. Calculated HOMO and LUMO values range from -7.6 to -7.9 eV and -1.7 to -2.3 eV. The molecular electrostatic potential in Fig. 5 shows the charge separation between the two ends within the molecule. The relatively more minor HOMO-LUMO gaps, hardness values, and more considerable chemical reactivity make molecule c more reactive. The molecules' larger electronegativity (χ) and

Table 3
Computed and experimentally measure vibrational data for molecules 1-8.

Molecules	Stretching Modes	Experimental Stretching frequencies in cm^{-1}	Computed Stretching frequencies in cm^{-1}
1	$\nu_{C=O}$	1660	1646
	ν_{O-H}	3320	3438
2	$\nu_{C=O}$	1675	1689
	ν_{O-H}	3330	3441
3	$\nu_{C=O}$	1694	1685
	ν_{N-H}	3321	3391
4	$\nu_{C=O}$	1678	1671
	ν_{O-H}	3390	3339
7	ν_{C-O}	1678	1672
	ν_{O-H}	3390	3334
8	$\nu_{C=O}$	1659	1698
	ν_{C-O}	1171	1192

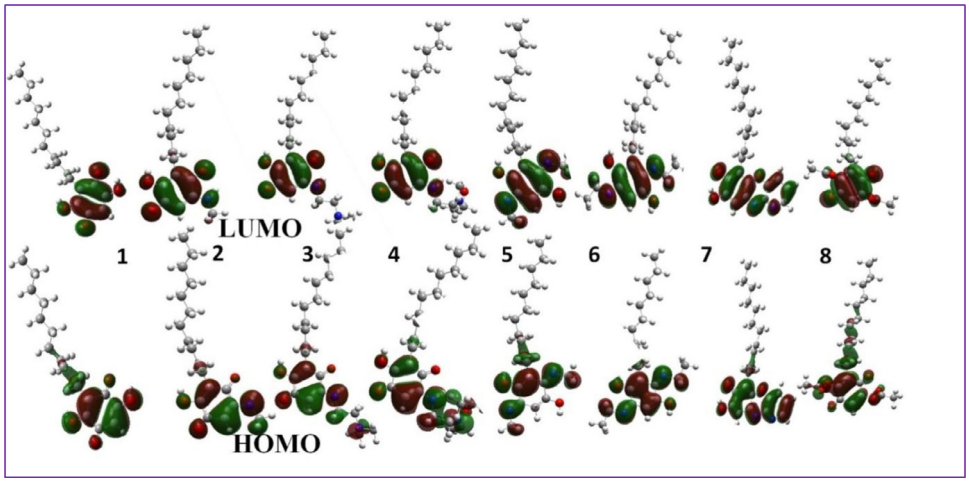

Fig. 4. Computed molecular orbital plots for synthesized molecules (1-8) with the counter value of 0.02 $Å^{-3}$.

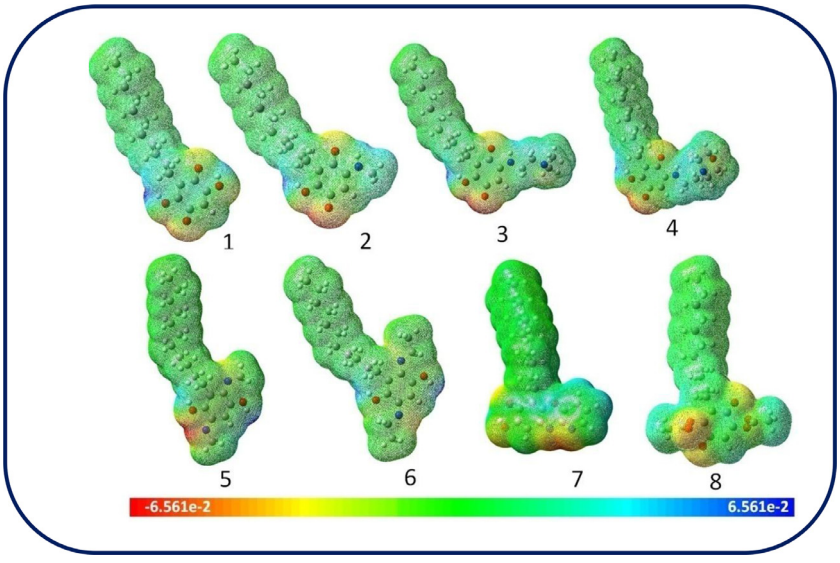

Fig. 5. Molecular electrostatic charge distribution plots for synthesized molecules (1-8) with an isovalue of 0.004. $Å^{-3}$.

electrophilicity index (ω) values suggest the binding mechanism towards their receptor. The molecule can bind with the receptor by donating the electron. The steric effect of longer chains is studied by recalculating the molecular geometries and electronic structures without the longer chain. The absence of a side-chain maintains a similar trend as synthesized molecules. The higher alkane chain can act as a hydrophobic unit and might help drug delivery.

The vibrational frequencies of experimental and theoretical values are analogous as illustrated in the Table 3. In compound **1** the C=O stretching vibrations are 1660 and 1646 cm^{-1} respectively and O-H stretching vibrations are appeared at 3320 and 3438

Table 4
The E_{HOMO}, E_{LUMO}, HOMO-LUMO gap (Δ), chemical hardness (η), electronegativity (χ) and electrophilicity index (ω) in eV for all the synthesized molecules 1-8.

Compounds	E_{HOMO}	E_{LUMO}	Δ	η	χ	ω
1	-8.62	-2.27	6.35	3.17	5.44	5.01
2	-7.71	-1.77	5.93	2.97	9.45	3.87
3	-7.63	-1.73	5.89	2.95	4.68	3.71
4	-7.68	-1.79	5.89	2.95	4.74	3.81
5	-7.49	-1.23	6.26	3.13	4.36	3.04
6	-7.53	-1.14	6.39	3.19	3.76	2.94
7	-7.86	-2.32	5.54	2.77	5.09	4.68
8	-9.25	-2.47	6.77	3.38	5.86	5.08

Table 5
In vitro COX-1, COX-2 inhibition activity of embelin hybrids (1-8).

Compounds	COX-1 IC_{50} (μM)[a]	COX-2 IC_{50} (μM)[a]	COX-2 S. I.[b]
1	6.42	2.98	2.15
2	6.54	3.10	2.11
3	3.58	1.65	2.17
4	3.18	1.54	2.06
5	7.65	2.56	2.98
6	6.85	2.15	3.18
7	3.19	1.56	2.04
8	2.25	1.23	1.83
Celecoxib	6.34	0.56	11.32
Ibuprofen	3.15	1.28	2.46

[a] The concentration of test compound produce 50% inhibition of COX-1, COX-2 enzyme, the result is the mean of two value obtained by assay of enzyme. [b]The *in vitro*COX-2 selectivity index (COX-1/COX-2).

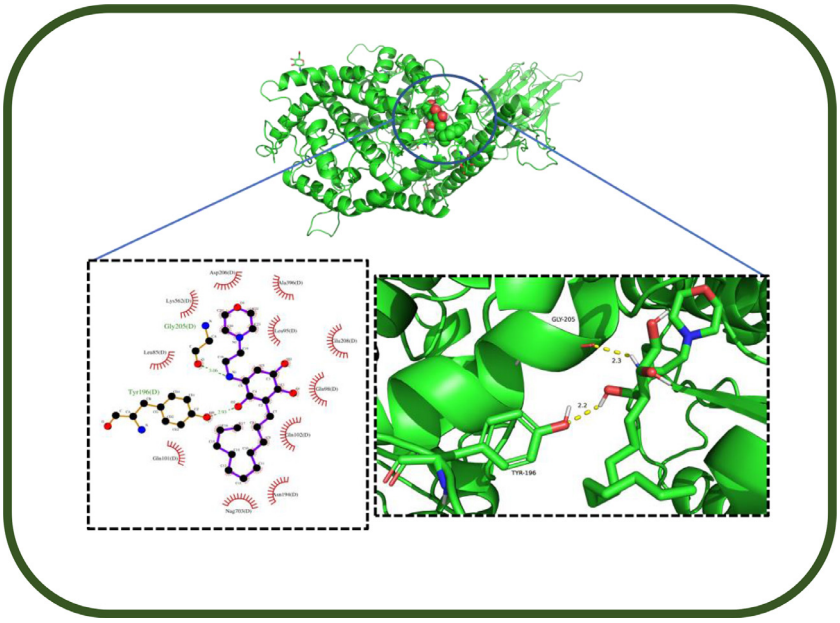

Fig. 6. Molecular docking interaction representation of **ligand 4** with omicron. a) 3D representation **ligand 4** (in stick) with omicron (molecular surface). b) 3D interaction of **ligand 4** in stick and amino acids forming hydrogen bond and hydrophobic interaction in line representation. c) LigPlot 2D interaction representation of **ligand 4** with protein.

cm^{-1} respectively. In compound **2** these vibrations are appeared at 1675 & 1689 cm^{-1} and 3330 & 3441 cm^{-1} respectively for CO and OH functions. In the compound **3** the vibrational frequencies for CO and OH functions appeared at 1694 & 1685 cm^{-1} and 3321 & 3391 cm^{-1} experimental and computational values respectively. The peaks at 1678 and 1671cm^{-1} for obtained and calculated vibrations due to CO stretching respectively and the peaks at 3390 and 3339 cm^{-1} due to for –OH functions for experimental and calculated values for compound **4**. In the compound **7** the vibrational frequencies for CO and OH functions appeared at 1678 & 1671 cm^{-1} and 3390 & 3334 cm^{-1} obtained and calculated values respectively. In the compound **8** the vibrational frequencies for COC and CO functions appeared at 1171 & 1192 cm^{-1} and 1659 & 1698 cm^{-1} experimental and computational values respectively.

The calculated values of E_{HOMO}, E_{LUMO}, HOMO-LUMO gap (Δ), chemical hardness (η), electronegativity (χ) and electrophilicity index (ω) in eV for all the synthesized molecules are shown in Table 4 .

3.3. In Vitro cyclooxygenase inhibition assay

The *in vitro* COX-1/COX-2 enzyme inhibitory activities determine the aptitude of examined embelin hybrids to inhibit ovine COX-1 and human recombinant COX-2 using an enzyme im-

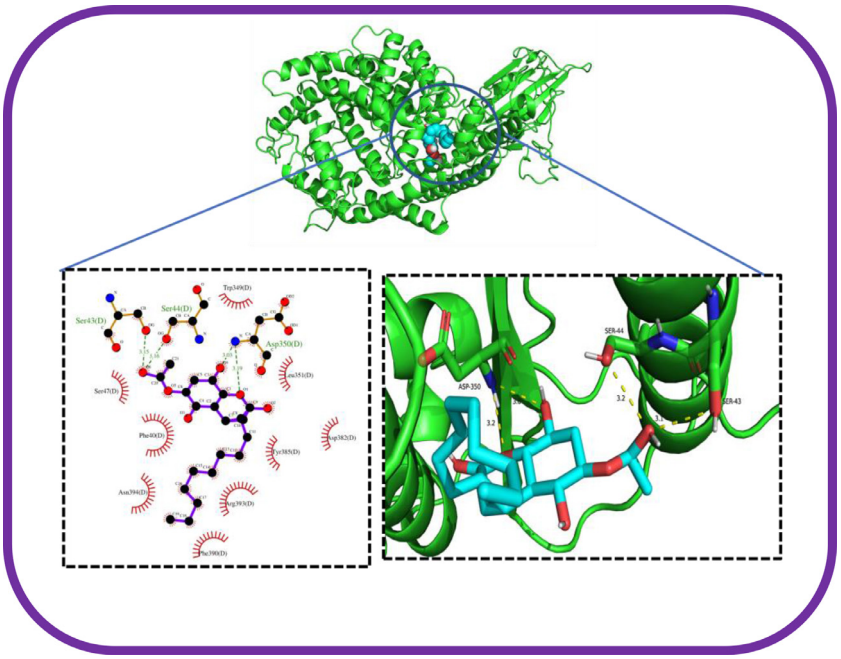

Fig. 7. Molecular docking interaction representation of **ligand 8** with omicron. a) 3D representation **ligand 8** (in stick) with omicron (molecular surface). b) 3D interaction of **ligand 8** in stick and amino acids forming hydrogen bond and hydrophobic interaction in line representation. c) LigPlot 2D interaction representation of **ligand 8** with protein.

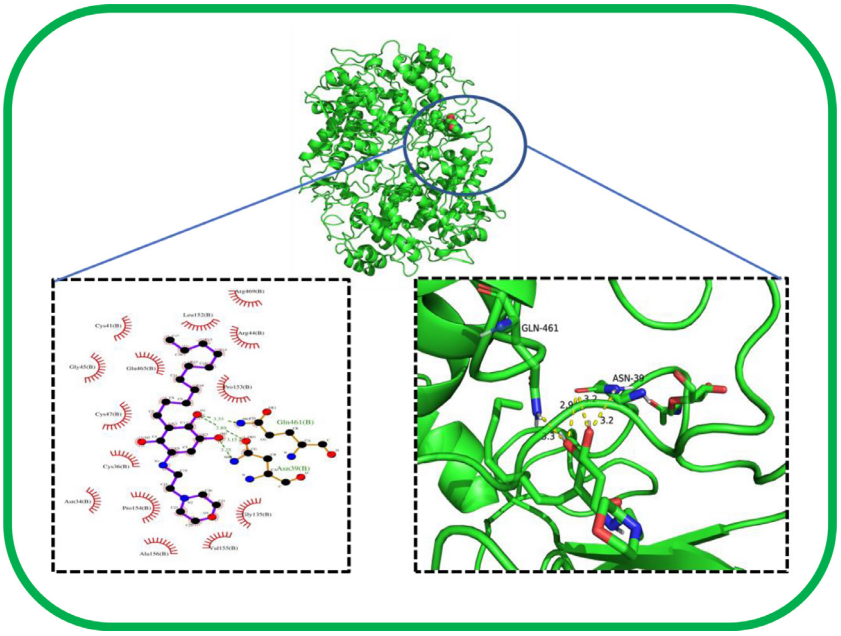

Fig. 8. Molecular docking interaction representation of **ligand 4** with COX-2. a) 3D representation **ligand 4** (in stick) with COX-2 (molecular surface). b) 3D interaction of **ligand 4** in stick and amino acids forming hydrogen bond and hydrohphobic interaction in line representation. c) LigPlot 2D interaction representation of **ligand 4** with protein.

munoassay (EIA). The consequences were (Table-5) exposed that the compounds **3, 4,** 7 and **8** were showed admirable COX-1 inhibitory activity with IC_{50} value 3.58, 3.18, 3.19 and 2.25μM respectively. While the compounds **3, 4,** 7 and **8**demonstrated excellent COX-2 inhibitory activities with IC_{50} value 1.65, 1.54, 1.56, and 1.23μMrespectively. In the same condition standard drugs Celecoxib and Ibuprofen showed IC_{50} 6.34 & 3.15μM for COX-1 and 0.56 μM & 1.28 μM for COX-2 respectively. Other compounds showed less to moderate cyclooxygenase inhibition activity as compared to standard drugs.

3.4. Molecular docking studies

The conformation that had the least binding affinity and most stability based on docking analysis was identified.

3.4.1. Docking study withSARS-CoV-2 Omicron virus variant (PDB ID:7T9L)

All the compounds **1-8** were taken for molecular docking study with SARS Cov-2 omicron variant and the standard drugs Celecoxib and Ibuprofen were used as reference.The conformation that had

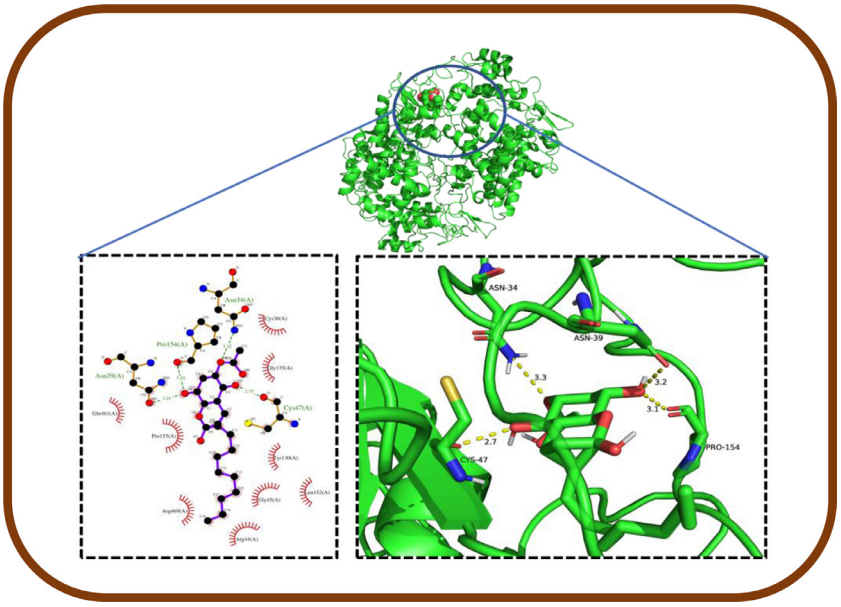

Fig. 9. Molecular docking interaction representation of **ligand 8** with COX-2. a) 3D representation **ligand 8** (in stick) with COX-2 (molecular surface). b) 3D interaction of **ligand 8** in stick and amino acids forming hydrogen bond and hydrohphobic interaction in line representation. c) LigPlot 2D interaction representation of **ligand 8** with protein.

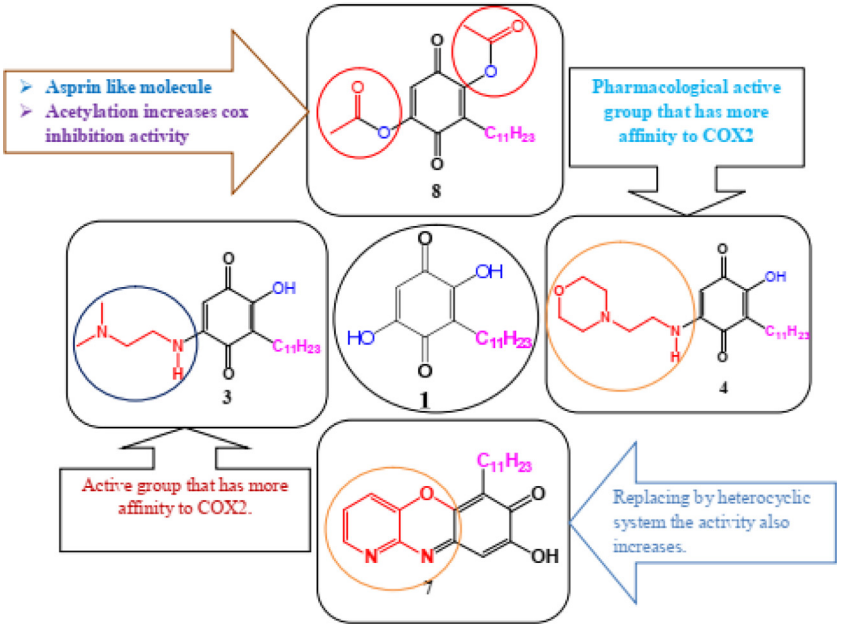

Fig. 10. The brief SAR study for synthesized embelin derivatives

the least binding affinity and most stability based on docking analysis was identified. *In silico* analysis revealed that the compounds**4** and **8** showed the best binding interactions with SARS-CoV-2 Omicron virus variant. Compound **4** formed two hydrogen bonds with Tyr196 and Gly205 amino acids (Fig. 6). Compound **8** formed four hydrogen bonds with Ser43, Ser44 and Asp350 amino acids (Fig. 7). Molecular docking results of the structures considered for docking with SARS-CoV-2 Omicron virus variant are depicted in the **Table-S1**.

3.4.2. Docking study with cyclooxygenase-2 (COX2) (PDB ID:6COX)

All the compounds **1-8** were taken for molecular docking study with SARS Cov-2 omicron variant and the standard drugs Celecoxib and Ibuprofen were used as reference. Bioinformatics analysis revealed that compounds**4** and **8**showed the best binding interactions with cyclooxygenase-2 (**PDB ID: 6COX**). Ibuprofen was observed to be having hydrophobic interactions with the -heme edge of cyclooxygenase-2.The compound **4** with a Vina score of -7.9kcal/mol and with forms two hydrogen bonds with ASN39, and GLN461 amino acids. Further, compound **8** showed strong interaction with the COX compared to the reference drug ibuprofen with a Vina score of -8.2kcal/mol and 4 exhibited four hydrogen bonds with ASN34, PRO154, ASN39 and CYS47. It can be noted that all the ligands are having interaction with both the proteins. Based on the vina score and number of hydrogen bonds and hydrophobic interactions 2D and 3D interaction diagrams for compound 4 and compound 8 is generated and shown in the Fig. 8 and 9 respectively (**Table-S2**).

4. Structure activity relationship studies

Embelin, a bioactive molecule, a combination of the hydrophilic-OH group, keto group, and hydrophobic aliphatic long chain, makes this molecule a perfect scaffold to develop drug candidates. In our previous study, we reported that the presence of OH, C=O, and an alkyl group in embelin is responsible for its strong binding to histone acetyl transferases, an enzyme involved in the post-translation modification referred to as histone acetylation. Replacement of the hydroxyl group by substituted amines and acetylation of the –OH function, the activity increases. Further, by the introduction of a heterocyclic system, activity increases. The brief SAR for synthesized compounds highlighted in Fig. 10.

5. Conclusion

In conclusion, we have lucratively intended and produced embelin hybrids in single-step reactions. The probable pharmacokinetic and pharmacodynamic properties of all the synthesized compounds were performed. The DFT calculations are used to compare the structure of the synthesized molecules. The anti-inflammatory activity studies of all the compounds (**1-8**) were carried out. In vitro, cyclooxygenase inhibition testing found that compounds **3**, **4**, **7**, and **8** are more effective inhibitors of COX-1 and COX-2 enzymes. Molecular docking study accessible the possible interactions between the synthesized compounds at the active situate of cyclooxygenase. The outcome is that some of the synthesized compounds bind with an enzyme in a very similar way to standard drugs. The imminent results in the current investigation could be obliged for the rising novel loom in developing embelin-containing anti-inflammatory drugs. Finally, from the SAR study, it has been suggested that acetyl and amine derivatives of embelin may be an excellent lead for further COX inhibition studies.

6. Author credit statement

All the authors have contributed and extended their support for making this manuscript to communicate for publications.

Declaration of Competing Interest

The authors declare that they have no known competing financialinterests or personal relationships that could have appeared to influence the work reported in this paper.

Data Availability

Data will be made available on request.

Acknowledgment

The authors are grateful to The Directors of IISc, Bengaluru, SAIF Punjab University, and CDRI, Lucknow for spectral data. For biological activities, the authors are grateful to The Director, Skanda Life Sciences Pvt. Ltd., Bengaluru. The thanks are due to Management, Indian Academy Degree College, Bengaluru for providing necessary facility for research work.

Supplementary materials

Supplementary material associated with this article can be found, in the online version, at doi:10.1016/j.molstruc.2022.134356.

References

[1] Samik Bindu, Somnath Mazumder, Uday Bandyopadhyay, Non-steroidal anti-inflammatory drugs (NSAIDs) and organ damage: a current perspective, Biochem. Pharmacol. 180 (2020) 114147, doi:10.1016/j.bcp.2020.114147.

[2] R Modak, J Basha, N Bharathy, K Maiti, P Mizar, A Bhat, K Suguna, R Taneja, TK. Kundu, Probing p300/CBP associated factor (PCAF)-dependent pathways with a specific small molecule inhibitor of lysine acetyltransferase, ACS Chem. Biol. 8 (2013) 1311–1323.

[3] S Srivastava, K Bhowmick, S Chatterjee, J Basha, TK Kundu, SK. Dhar, Histone H3K9 acetylation level modulates gene expression and may affect parasite growth in human malaria parasite plasmodium falciparum, FEBS J. 281 (23) (2014) 5265–5278 Dec, doi:10.1111/febs.13067.

[4] N.J. Basha, S.M. Basavarajaiah, S. Baskaran, P. Kumar, A comprehensive insight on the biological potential of embelin and its derivatives, Nat. Prod. Res. 36 (12) (2022) 3054, doi:10.1080/14786419.2021.1955361.

[5] K Sumalatha, M Gowda, S. Meenakshisundaram, ROS-mediated induction of apoptosis by benzoquinone embelin in human colon adenocarcinoma cells HT-29, J. Complement. Integr. Med. 14 (2) (2017) 20160131.

[6] C Xu, B Zheng, J Pei, S Shen, J. Wang, Embelin induces apoptosis of human gastric carcinoma through inhibition of p38 mapk and nf-κb signaling pathways, Mol. Med. Rep. 14 (1) (2016) 307–312.

[7] S. Zappavigna, A.M. Cossu, A. Grimaldi, M. Bocchetti, G.A. Ferraro, G.F. Nicoletti, R. Filosa, M. Caraglia, Anti-inflammatory drugs as anticancer agents, Int. J. Mol. Sci. 21 (7) (2020) 2605.

[8] IS Lee, DH Cho, KS Kim, KH Kim, J Park, Y Kim, JH Jung, K Kim, HJ Jung, HJ. Jang, Anti-inflammatory effects of embelin in A549 cells and human asthmatic airway epithelial tissues, Immunopharmacol. Immunotoxicol 40 (1) (2018) 83–90, doi:10.1080/08923973.2017.1414836.

[9] S Mahendran, S Badami, S Ravi, Veerapur V.P ThippeswamyBS, Synthesis and evaluation of analgesic and anti-inflammatory activities of most active free radical scavenging derivatives of embelin-A structure-activity relationship, Chem. Pharm. Bull. 59 (8) (2011) 913–919.

[10] K. Bezu, D. Bistrat, K Asres, In vivo antimalarial evaluation of embelin and its semi-synthetic aromatic amine derivatives, Pharmacogn. J. 7 (2015) 305–310.

[11] G. Viault, K.S. Babu, F. Gautier, S. Barillé-Nion, P. Juin, O. Tasseau, R. Grée, Hemisynthesis of selected embelin analogs and investigation of their proapoptotic activity against cancer cells, Med. Chem. 9 (2013) 1028–1034.

[12] Y Liu, XD Chen, J Yu, JL Chi, FW Long, HW Yang, KL Chen, ZY Lv, B Zhou, ZH Peng, XF Sun, Y Li, ZG. Zhou, Deletion of xiap reduces the severity of acute pancreatitis via regulation of cell death and nuclear factor-κB activity, Cell Death. Dis. 8 (3) (2017) e2685, doi:10.1038/cddis.2017.70.

[13] G Sethi, S Chatterjee, P Rajendran, F Li, MK Shanmugam, KF Wong, AP Kumar, P Senapati, AK Behera, KM Hui, J Basha, N Natesh, JM Luk, TK. Kundu, Inhibition of STAT3 dimerization and acetylation by garcinol suppresses the growth of human hepatocellular carcinoma in vitro and in vivo, Mol. Cancer 13 (2014) 66, doi:10.1186/1476-4598-13-66.

[14] F Li, MK Shanmugam, L Chen, S Chatterjee, J Basha, AP Kumar, TK Kundu, G. Sethi, Garcinol, a polyisoprenylated benzophenone modulates multiple proinflammatory signaling cascades leading to the suppression of growth and survival of head and neck carcinoma, Cancer Prev. Res. (Phila.) 6 (8) (2013) 843–854 Aug, doi:10.1158/1940-6207.CAPR-13-0070.

[15] M Guha, S Srinivasan, K Guja, E Mejia, M Garcia-Diaz, FB Johnson, G Ruthel, BA Kaufman, EF Rappaport, MR Glineburg, JK Fang, AJ Klein-Szanto, A Klein Szanto, H Nakagawa, J Basha, T Kundu, NG Avadhani, HnRNPA2 is a novel histone acetyltransferase that mediates mitochondrial stress-induced nuclear gene expression, Cell Discov. 2 (2016) 16045, doi:10.1038/celldisc.2016.45.

[16] N. Jeelan Basha, N.M. Goudgaon, A comprehensive review on pyrimidine analogs-versatile scaffold with medicinal and biological potential, J. Molecul. Struct. 1246 (2021) 131168.

[17] N. Jeelan Basha, S.M. Basavarajaiah, K Shyamsunder, Therapeutic potential of pyrrole and pyrrolidine analogs: an update, Mol. Divers. (2022) 1–23, doi:10.1007/s11030-022-10387-8.

[18] B.S. Mathada, N.G. Yernale, J.N. Basha, J. Badiger, An insight into the advanced synthetic recipes to access ubiquitous indole heterocycles, Tetrahedron Lett. 85 (2021) 153458, doi:10.1016/j.tetlet.2021.153458.

[19] G.Y. Nagesh, Mohammad Javeed, Jeelan N Basha, K. Prashantha, R. Nithin, P.R. Thanushree, S. Vivekananda, H.B. Siri S.Gowda, S.M. Punarva, Basavarajaiah, design, spectral analysis, dft calculations, antimicrobial, anti-TB, antioxidant activity and molecular docking studies of novel bis-benzoxazines with cytochrome c peroxidase, J. Mol. Struct. 1262 (2022) 132977, doi:10.1016/j.molstruc.2022.132977.

[20] S.M. Basavarajaiah, Nagesh GY, M Javeed, R Bhat, S Nethravathi, Jeelan N. Basha, KR Reddy, C Nisarga, P Srinivas, Synthesis, spectral analysis, dft calculations, biological potential and molecular docking studies of indole appended pyrazolo-triazine, Mol. Divers (2022), doi:10.1007/s11030-022-10448-y.

[21] NM Goudgaon, NJ Basha, SB. Patil, Synthesis and antimicrobial evaluation of 5-iodopyrimidine analogs, Indian J. Pharm. Sci. 71 (6) (2009) 672–677 Nov, doi:10.4103/0250-474X.59551.

[22] Basavarajaiah SuliphuldevaraMatada, Nagesh Gunavanthrao Yernale, Jeelan N Basha, Updates on the versatile quinoline heterocycles as anticancer agents, Phys. Sci. Rev. (2021) 000010151520210040, doi:10.1515/psr-2021-0040.

[23] Basavarajaiah Suliphuldevara Mathada, Sasidhar B. Somappa, An insight into the recent developments in anti-infective potential of indole and associated hybrids, J. Mol. Struct. 1261 (2022) 132808, doi:10.1016/j.molstruc.2022.132808.

[24] a). N. Jeelan Basha, S.M. Basavarajaiah, Anticancer potential of bioactive molecule luteolin and its analogs: an update, Polycyclic Aromat. Compd. (2022). DOI:, doi:10.1080/10406638.2022.2080728; b). N.Jeelan Basha, S.M. Basavarajaiah, An insight into therapeutic efficacy of heterocycles as hi-

stone modifying enzyme inhibitors that targets cancer epigenetic pathways, Chem. Biol. Drug Des. (2022), doi:10.1111/cbdd.14135.

[25] a). B.H.M. Mruthyunjayaswamy, B.K. Shanthaveerappa, S.M. Basavarajaiah, J. Indian Chem. Soc. 87 (2010) 1109; b). S.M. Basavarajaiah, B.H.M. Miuthyunjayaswamy, Synthesis and anti-microbial activity of some new5-substituted-n1-[(1e)-(2-hydroxyquinolin-3-yl)methylene]-3-phenyl-1h-indole-2-carbohydrzide derivatives, Heterocycl. Commun. 15 (3) (2009) 217–224, doi:10.1515/HC.2009.15.3.217.

[26] a). Basavarajaiah Suliphuldevara Matada, Nagesh Gunavanthrao Yernale and Mohammad Javeed, Design, spectroscopic studies, dft calculations and evaluation of biological activity of novel 1,3-Benzoxazines encompassing isoniazid, Polycyclic Aromat. Compd., 2021. DOI: 10.1080/10406638.2021.2019062b). B. S. Mathada (2022) Polycyclic Aromatic Compounds, https://doi.org/10.1080/10406638.2022.2089177

[27] a). T. Yanai, D. Tew, N. Handy, A new hybrid exchange-correlation functional using the coulomb-attenuating method (CAM-B3LYP), 2004 Chem. Phys. Lett., 393 51–57; b). R.G. Parr, W. Yang, Density Functional Theory of Atoms and Molecules Oxford University Press, New York, NY, USA, 1989; c). R.G. Pearson, Chemical Hardness Wiley-VCH, Weinheim, Germany, 1997; d). R.G. Parr, R.A. Donnelly, M. Levy, W.E.Electronegativity Palke, The density functional viewpoint, 1978 J. Chem. Phys., 68 3801–3808; e). R.G. Parr, R.G. Pearson, Absolute hardness: companion parameter to absolute electronegativity, 1983 J. Am. Chem. Soc., 105 7512–7516; f). R.G. Parr, L.V. Szentpály, S.Electrophilicity index Liu, 1999 J. Am. Chem. Soc., 121 1922–1924.

[28] H. Suryavanshi, R.D. Chaudhari, V. Patil, et al., Design, synthesis and docking study of vortioxetine derivatives as a SARS-CoV-2 main protease inhibitor, DARU J. Pharm. Sci. 30 (2022) 139–152, doi:10.1007/s40199-022-00441-z.

[29] S.M. Basavarajaiah, B.H.M Mruthyunjayaswamy, Pharmacological activities of 6-substituted-3-(5-chloro-3-phenyl-1*H*-indole-2yl)-3, 4-dihydro-4-substituted-4-substituted-phenacyl-2*H*-1, 3-benzoxazin-2-ones, inter. J. Sci. Res 9 (7) (2020) 518–521.

[30] S.M. Basavarajaiah, B.H.M. Mruthyunjayaswamy, Pharmacological activities of some 5-Substituted-3-phenyl-N_{β}-(substituted- 2-oxo-2H-pyrano [2, 3-b] quinoline-3- carbonyl)-1H-indole-2-carboxyhydrazides, Der. Pharmacia Sinica 12 (5) (2021) 011, doi:10.36648/0976-8688.21.12.011.

[31] S.M. Basavarajaiah, B.H.M. Mruthyunjayaswamy, Pharmacological activities of 5-substituted-N-(substituted-2H-[1, 3] oxazino [6, 5-b] quinolin-3 (4H)-yl)-3-phenyl-1H-indole-2-carboxamides, Int. J. Creative Res. Thoughts 8 (2020) 232–236.

[32] Khaled R.A. Abdellatif, Wael A.A. Fadaly, Waleed A.M.Ali &Gehan M.Kamel, Synthesis, cyclooxygenase inhibition, anti-inflammatory evaluation and ulcerogenicliability of new 1,5-diarylpyrazole derivatives, J. Enzyme Inhib. Med. Chem. 31 (3) (2016) 54–60, doi:10.1080/14756366.2016.1201815.

[33] Noel M O'Boyle, et al., Open babel: an open chemical toolbox, J. cheminformatics 3 (2011).

[34] E.J. Murphy, C.L. Metcalfe, J. Basran, P.C. Moody, E.L. Raven, Biochemistry 47 (2008) 13933–13941, doi:10.1021/bi801480r.

[35] DeLano, W. L. (2002). PyMOL

[36] R.A. Laskowski, M.B. &Swindells, J. Chem. Inf. Model. 51 (10) (2011) 2778–2786, doi:10.1021/ci200227u.

[37] F Caruso, M Rossi, JZ Pedersen, S. Incerpi, Computational studies reveal mechanism by which quinone derivatives can inhibit SARS-CoV-2. study of embelin and two therapeutic compounds of interest, methyl prednisolone and dexamethasone, J. Infect. Public Health 13 (12) (2020) 1868–1877 Dec, doi:10.1016/j.jiph.2020.09.015.